

## Second-order nature of the spin-reorientation phase transition in $\text{SmCrO}_3$

G. Gorodetsky\*

*Department of Physics, Ben-Gurion University of the Negev, Beer-Sheva, Israel  
and Department of Electronics, The Weizmann Institute of Science, Rehovot, Israel*

R. M. Hornreich

*Department of Electronics, The Weizmann Institute of Science, Rehovot, Israel*

S. Shaft\*

*Department of Physics, Ben-Gurion University of the Negev, Beer-Sheva, Israel*

B. Sharon

*Department of Electronics, The Weizmann Institute of Science, Rehovot, Israel*

A. Shaulov\*

*Department of Physics, Ben-Gurion University of the Negev, Beer-Sheva, Israel*

B. M. Wanklyn

*Clarendon Laboratory, Oxford, England*

(Received 27 August 1976)

The spin-reorientation phase transition in  $\text{SmCrO}_3$  at  $T \approx 33^\circ\text{K}$  is studied using acoustic-velocity and specific-heat measurements. Although the reorientation occurs within a narrow temperature region ( $\sim 1^\circ\text{K}$ ) the acoustic data show clearly that the process is a continuous one, involving two second-order phase transitions. All the observed effects, including those induced by externally applied magnetic fields are satisfactorily accounted for using a phenomenological model with magnetoelastic coupling terms. The thermal anomaly associated with the spin reorientation is also observed and used to calculate the uniaxial energy of the chrome spin system.

### I. INTRODUCTION

The compound  $\text{SmCrO}_3$ , in conformity with other rare-earth orthochromites, crystallizes in an orthorhombically distorted perovskite structure (space group  $Pbmm$ ) with four formula units per unit cell.<sup>1</sup> In these compounds the exchange coupling between the magnetic moments of the  $\text{Cr}^{3+}$  nearest neighbors is predominantly antiferromagnetic and they order in a predominantly  $G$ -type spin mode.<sup>2</sup> A characteristic feature of this spin mode is the appearance of weak ferromagnetism, resulting from a small canting from the antiferromagnetic axis.

Four of the rare-earth orthochromites,  $\text{ErCrO}_3$ ,<sup>3</sup>  $\text{NdCrO}_3$ ,<sup>4</sup>  $\text{SmCrO}_3$ ,<sup>5,6</sup> and  $\text{GdCrO}_3$ ,<sup>7,8</sup> exhibit a spontaneous reorientation of the magnetically ordered spin system.<sup>9</sup> In  $\text{SmCrO}_3$ , for example, the  $\text{Cr}^{3+}$  antiferromagnetic axis coincides with the orthorhombic  $a$  axis immediately below  $T_N = 190^\circ\text{K}$ . At approximately  $33^\circ\text{K}$  the magnetic structure changes spontaneously and the  $\text{Cr}^{3+}$  antiferromagnetic axis rotates from the  $a$  to the  $c$  axis. This process is apparent in the single-crystal magnetization and susceptibility measurements reported by Yaeger<sup>6</sup> and reproduced in Fig. 1. We see that the change in the direction of the bulk

magnetization occurs within a narrow temperature region, approximately  $1^\circ\text{K}$  in width, and that the  $a$  and  $c$  axis susceptibilities each exhibit an anomalous peak at the high- and low-temperature end points, respectively, of this process. The occurrence of such susceptibility peaks at the end points of the transition region is indicative of two second-order phase transitions, associated with the rotation of the antiferromagnetic axis from one symmetry axis to another.<sup>10</sup> Although common in the orthoferrites,<sup>11</sup> this was the first indication of continuous spin-reorientation in an orthochromite. (There is evidence<sup>7,8</sup> that the reorientation process in  $\text{GdCrO}_3$  is also a continuous one.)

The central objective of our study was to determine whether the spin-reorientation process in  $\text{SmCrO}_3$  is indeed continuous. Two experimental techniques were employed for this purpose: acoustic-velocity and specific-heat measurements. Acoustic measurements are particularly suited for this purpose as inelastic-scattering experiments on similar compounds<sup>12</sup> have shown that the acoustic branch of the spin-wave spectrum becomes soft at the end points of a continuous rotation process. Since critical fluctuations are negligible at such displacive-type phase transitions, the interaction between phonons and this soft mode

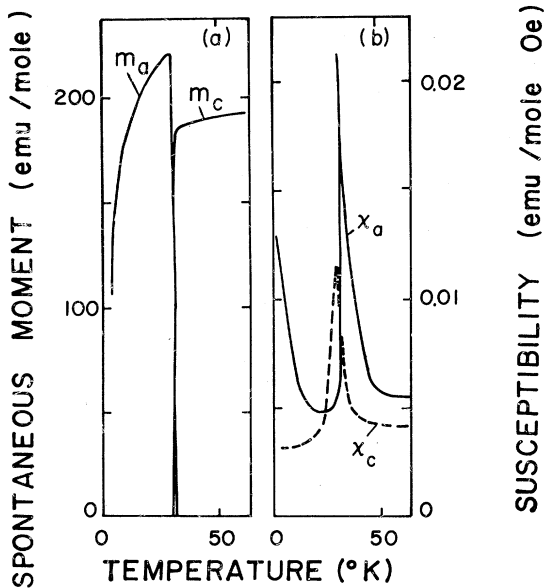


FIG. 1. Temperature dependence of (a) magnetization and (b) susceptibility parallel to the  $a$  and  $c$  crystallographic axes of  $\text{SmCrO}_3$  in the spin-reorientation region, as measured by Yaeger (Ref. 6).

is essentially of a resonant nature and manifests itself in characteristic anomalies in the elastic constants. The form of these anomalies is dependent upon the nature of the magnetoelastic interaction. Thus it is known<sup>13</sup> that a magnetoelastic coupling term, linear in the order parameter of the phase transition, results in resonant dips in the elastic constants whereas terms quadratic in the order parameter lead to steplike discontinuities. These resonant interactions can be examined further by applying an external magnetic field in the  $a$ - $c$  crystallographic plane. The presence of such a field has two effects, a shift of the transition temperatures and a suppression of soft modes.<sup>14</sup> These effects have been observed by us. They are analyzed using a phenomenological free-energy model which includes a magnetoelastic coupling linear in the strain. This model has been used previously<sup>14,15</sup> in acoustic studies of continuous spin-reorientation-type phase transitions in  $\text{ErFeO}_3$  and  $\text{TmFeO}_3$ .

The purpose of the specific-heat measurements was twofold: First, to confirm the second-order character of the spin reorientation process, and second, to obtain quantitative data on the magnetic interactions responsible for the phase transition.

## II. EXPERIMENTAL RESULTS

The single crystals of  $\text{SmCrO}_3$  used in our work were grown by the flux method.<sup>16</sup> For the acoustic

measurements, a  $5.5 \times 5 \times 3$  mm crystal, with its longest dimension coinciding with the crystallographic  $c$  axis, was chosen. Sound wave propagation at 30 MHz was studied by a phase-comparison single-echo technique described in detail elsewhere.<sup>17</sup> The echo pattern showed several echoes at liquid-nitrogen temperature, but deteriorated in the vicinity of the phase-transition temperatures. The velocity resolution was better than 100 ppm and the temperature stability better than  $\pm 0.02$  °K. The absolute accuracy of the temperature measurement was  $\pm 1$  °K.

Three different sound wave propagation modes were studied. (a) Shear waves propagating along the  $c$  axis, polarized parallel to the  $a$  axis: The results obtained are summarized in Fig. 2. Two pronounced dips of about 3% in the sound velocity were observed, corresponding to the transition end points  $T_l$  and  $T_u$ . The effect of a 1-kOe magnetic field applied along the  $c$  axis on the shear velocity is shown in Fig. 3. We see that the dip corresponding to  $T_l$  is suppressed and that both dips are shifted toward lower temperatures. The effect of magnetic fields applied along the  $a$  axis on the shear velocity is shown in Fig. 4. Here both of the shear velocity dips are shifted toward higher temperatures and there is a suppression of the dip corresponding to  $T_u$ . (b) Shear waves prop-

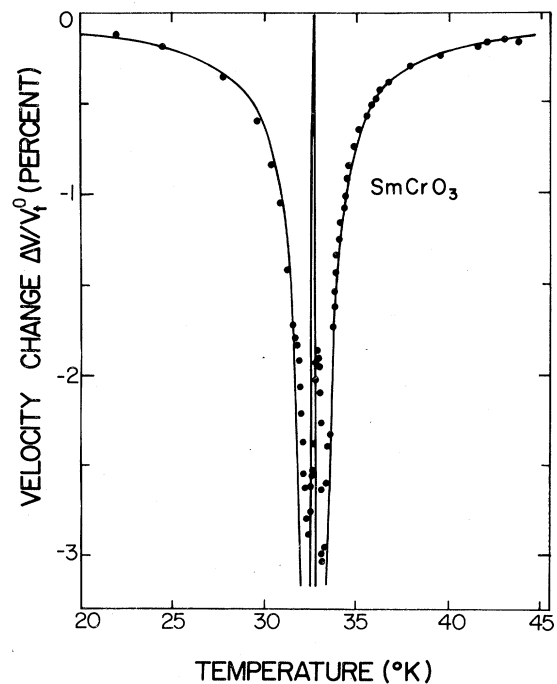


FIG. 2. Temperature dependence of velocity changes of a 30-MHz shear wave, propagating along the  $c$  axis and polarized parallel to  $a$ . The solid line is the theoretical best-fit curve.

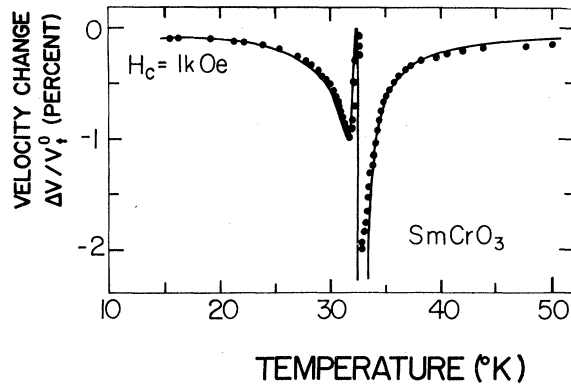


FIG. 3. Temperature dependence of velocity changes of a 30-MHz shear wave, propagating along the  $c$  axis and polarized parallel to  $a$ . The magnetic field  $H_c$  is applied along the  $c$  axis. The solid line is the theoretical best-fit curve.

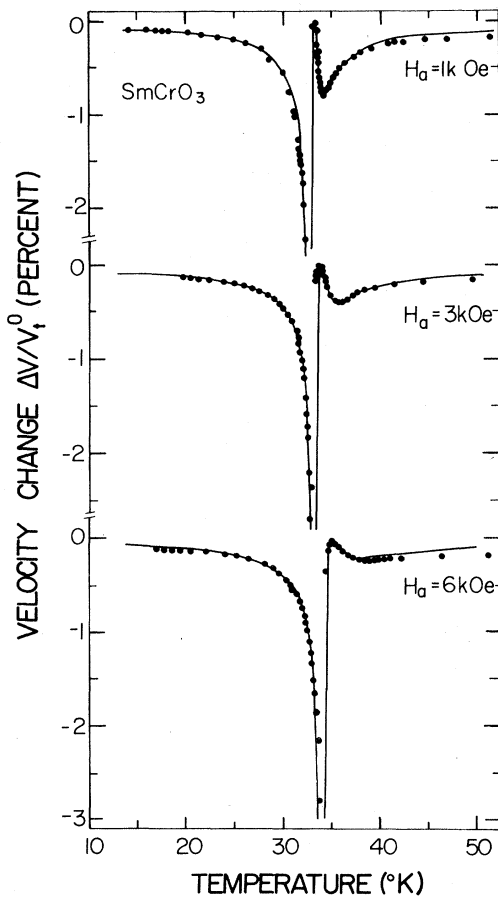


FIG. 4. Temperature dependence of velocity changes of a 30-MHz shear wave, propagating along the  $c$  axis and polarized parallel to  $a$ . The magnetic field  $H_a$  is applied along the  $a$  axis. The solid lines are theoretical best-fit curves.

agating along the  $c$  axis, but now polarized along the  $b$  axis: The experimental results are shown in Fig. 5(a). No significant anomaly was observed in the phase-transition region. (c) Longitudinal waves propagating along the orthorhombic  $c$  axis: The experimental velocity changes as a function of temperature are shown in Figs. 5(b) and 5(c). A single velocity dip of about 0.3% was observed in the transition region.

The velocities at  $T = 300^\circ\text{K}$  were  $V_l^0 = (7.00 \pm 0.07) \times 10^5$  cm/sec for longitudinal waves and  $V_s^0 = (3.55 \pm 0.04) \times 10^5$  cm/sec for shear waves polarized along the  $a$  axis.

For the specific heat measurements several small crystals, each approximately  $1\text{ mm}^3$  in volume, were glued together using a G.E. varnish with a high thermal conductivity. The total weight of the aggregate was 1.5 g. Measurements were carried out in an adiabatic calorimeter using a continuous-heating technique. The temperature was raised at an average rate of  $0.2^\circ\text{K}/\text{min}$  and data points were recorded at temperature intervals of  $0.2^\circ\text{K}$  from 22 to  $54^\circ\text{K}$ . The temperature was measured with a  $100\text{-}\Omega$  ambient-resistance Rosemount 118F miniature platinum resistor. The absolute temperature accuracy was  $\pm 1^\circ\text{K}$ . Details of the experimental apparatus will be given elsewhere.

The results of the specific-heat measurements

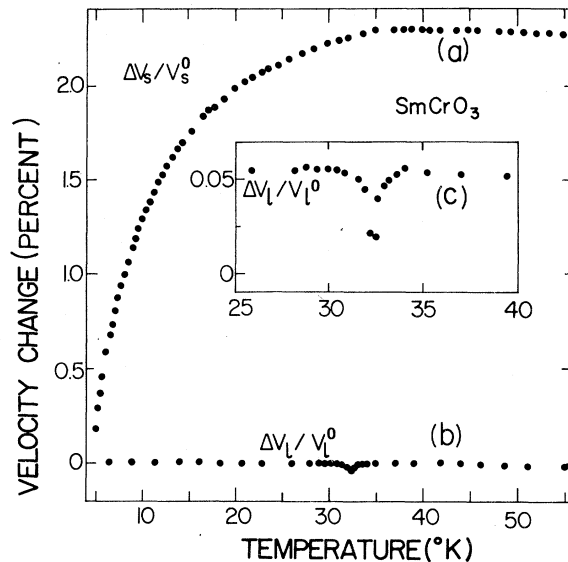


FIG. 5. Temperature dependence of (a) velocity changes of a 30-MHz shear wave, propagating along the  $c$  axis and polarized parallel to  $b$ ; (b) velocity changes of a 30-MHz longitudinal wave, propagating along the  $c$  axis; (c) velocity changes of a 30-MHz longitudinal wave, propagating along the  $c$  axis in and near the spin-reorientation region.

are given in Fig. 6. Also reproduced in the figure are the  $T < 20$  °K results of de Combarieu *et al.*<sup>18</sup> The anomaly between 33 and 35 °K is clearly evident.

### III. ANALYSIS

It has been shown<sup>13</sup> that a conventional free-energy model is applicable to the analysis of the static magnetoelastic properties associated with a coherent rotation of the spin system. In this model, the zero-field free-energy density includes a magnetic anisotropy term  $F_k$ , a magnetoelastic coupling term  $F_{me}$ , and the elastic energy  $F_e$ . The expressions pertinent to the propagation geometry employed in this study are

$$\begin{aligned} F_k &= \frac{1}{2}K_u \cos 2\theta + K_b \cos 4\theta, \\ F_{me} &= 2\epsilon_{zz}(B_{33} - B_{31}) \sin^2\theta - \epsilon_{xz}B_{55} \sin 2\theta, \\ F_e &= \frac{1}{2}C_{33}^0 \epsilon_{zz}^2 + \frac{1}{2}C_{55}^0 \epsilon_{xz}^2 + \frac{1}{2}C_{44}^0 \epsilon_{yz}^2. \end{aligned} \quad (1)$$

Here  $K_u$  and  $K_b$  are twofold and fourfold anisotropy coefficients, due to crystalline anisotropy and the coupling between the chrome and rare-earth spin systems.  $\theta$  is the angle between the antiferromagnetic and the  $a$  axes;  $\epsilon_{ij}$  are strain components;  $C_{ij}^0$  are normal elastic constants; and  $(B_{33} - B_{31})$ ,  $B_{55}$  are magnetoelastic coupling coefficients. Higher-order terms in the magnetoelastic coupling energy can be neglected.

The spontaneous spin reorientation is due to the different temperature dependence of  $K_u$  and  $K_b$ .<sup>10,19</sup> Since the effect of the coupling term  $F_{me}$

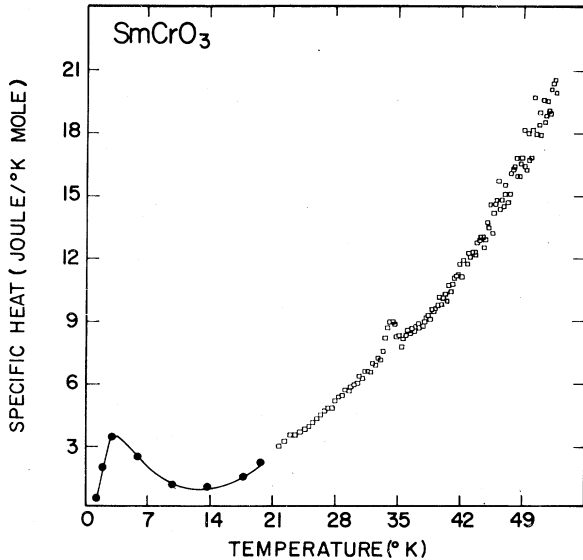


FIG. 6. Specific heat of  $\text{SmCrO}_3$  vs temperature. The data below 20 °K are taken from de Combarieu *et al.* (Ref. 18).

is negligible, the angular dependence of the magnetization in the spin-reorientation region  $T_1 \leq T \leq T_u$  is obtained from the equilibrium condition  $\partial F_k / \partial \theta = 0$ . This gives

$$\cos 2\theta = -K_u / 8K_b, \quad T_1 \leq T \leq T_u, \quad (2)$$

where the transition temperatures  $T_u$  and  $T_1$  correspond to  $\theta = 0$  and  $\theta = \frac{1}{2}\pi$ , respectively.

In the presence of an external magnetic field, we must supplement the free-energy density terms in Eq. (1) by

$$F_h = - \sum_{i=1}^2 \vec{M}_i \cdot \vec{H} - \sum_{i,j=1}^2 \vec{M}_i \cdot \vec{D}_{ij} (\vec{\chi}_j^R \vec{H}). \quad (3)$$

This expression consists of Zeeman term, in which  $\vec{M}_i$  ( $i = 1, 2$ ) denotes  $\text{Cr}^{3+}$  sublattice magnetizations and  $\vec{H}$  denotes the applied magnetic field, and a term due to the coupling between the  $\text{Cr}^{3+}$  spin system and the polarized rare-earth ions. This latter term has been written in a two-sublattice molecular-field approximation,<sup>20</sup> in which  $\vec{D}_{ij}$  is the coupling tensor and  $\vec{\chi}_j^R$  is the susceptibility tensor of each rare-earth sublattice. The indices  $i, j$  refer to  $\text{Cr}^{3+}$  and rare-earth sublattices, respectively. Since the entropy change associated with the rotation of the magnetically ordered system is negligible,<sup>14,21</sup> we can omit the spin-entropy term from the free-energy in the present analysis. We also omit the contribution to the free-energy due to rare-earth-rare-earth interaction terms; this contribution is of minor importance whenever the spin reorientation takes place at temperatures well above those at which cooperative rare-earth ordering occurs.<sup>22</sup> For the case of  $\text{SmCrO}_3$ , we have seen that the reorientation is at approximately 33 °K, while  $\text{Sm}^{3+}$  ordering in isomorphous  $\text{SmAlO}_3$  occurs at 1.3 °K.<sup>18</sup>

The effective elastic constants  $C_{ij}$  in the spin reorientation region are derived from the total free-energy density

$$F(\epsilon_{ij}, \theta(\epsilon_{ij})) = F_m + F_{me} + F_e + F_h, \quad (4)$$

by means of the equilibrium condition  $(\partial F / \partial \theta)_{\epsilon_{ij}} = 0$ . We obtain

$$C_{ij} = C_{ij}^0 - \left[ \frac{\partial}{\partial \epsilon_{ij}} \left( \frac{\partial F}{\partial \theta} \right)_{\epsilon_{ij}} \right]_{\theta}^2 / \left( \frac{\partial^2 F}{\partial \theta^2} \right)_{\epsilon_{ij}}, \quad (5)$$

where  $C_{ij} = \partial^2 F / \partial \epsilon_{ij}^2$  and  $C_{ij}^0 = (\partial^2 F / \partial \epsilon_{ij}^2)_{\theta}$ . The second derivative  $(\partial^2 F / \partial \theta^2)_{\epsilon_{ij}}$  is proportional to the square of the soft-mode frequency.<sup>13</sup> The velocity change of a given sound wave in the spin-reorientation region is a consequence of the change in the appropriate elastic constants. For the geometries employed in our study, we have the following:

- (a) Shear wave propagating along the  $c$  axis,

polarized parallel to  $a$ : The relative velocity change, as obtained from Eqs. (1) and (3)–(5), is

$$\frac{\Delta V}{V_t^0} = - \frac{2B_{55}^2 \cos^2 2\theta}{\rho(V_t^0)^2 (\partial^2 F / \partial \theta^2)_{\epsilon_{xz}}}, \quad (6)$$

where  $\rho = 7.35 \text{ g/cm}^3$  is the x-ray density<sup>1</sup> and  $\rho(V_t^0)^2 = C_{55}^0$ . A least-squares fit of Eq. (6) to the experimental results yielded the following parameter values:  $B_{55}^2/K_b = 4.4 \times 10^{11} \text{ erg/cm}^3$ ,  $T_l = 32.4 \text{ K}$ , and  $T_u = 32.9 \text{ K}$ . It was assumed that  $K_u$  is linearly dependent on the temperature and that  $K_b$  is constant in the spin-reorientation region. This has been found previously to be a fairly good approximation.<sup>13,15</sup> The calculated velocity shift for  $\vec{H} = 0$  is shown in Fig. 1. It is in excellent agreement with the experimental data.

The effect of an external magnetic field on the velocity change was studied experimentally by applying fields  $H_c$  and  $H_a$  along the orthorhombic  $c$  and  $a$  axes, respectively. In an applied field  $H_c$  the free-energy density becomes<sup>15</sup>

$$F_c = \frac{1}{2} K_u \cos 2\theta + K_b \cos 4\theta - \epsilon_{xz} B_{55} \sin 2\theta + \frac{1}{2} C_{55}^0 \epsilon_{xz}^2 - m H_c \cos \theta - 2 H_c \chi_{cc}^R H_c^R \cos \theta. \quad (7)$$

The final term in Eq. (7) is, as discussed earlier, due to the chrome–rare-earth coupling. In this expression,  $\vec{m} = \vec{M}_1 + \vec{M}_2$  denotes the  $\text{Cr}^{3+}$  weak ferromagnetic moment,  $\chi_{cc}^R$  is the susceptibility of the rare-earth ions parallel to the  $c$  axis, and  $H_c^R$  is the  $\Gamma_4(F_2)$  configuration effective field exerted by the ordered  $\text{Cr}^{3+}$  spin system acting on the rare-earth ions.<sup>23</sup>

Theoretical velocity-change curves were calculated using Eqs. (6) and (7) and the  $\vec{H} = 0$  best-fit parameters given above. The best-fit curve, obtained with  $(m + 2\chi_{cc}^R H_c^R)/K_b = 1.92 \times 10^{-2} \text{ Oe}^{-1}$ , is shown in Fig. 3. The agreement with the experimental data is excellent.

The effective field  $H_c^R$  in  $\Gamma_2(F_x)$ -phase  $\text{SmCrO}_3$ ,<sup>6</sup> and in the isomorphous and magnetically similar compounds  $\text{ErCrO}_3$ ,<sup>3</sup> and  $\text{TmCrO}_3$ ,<sup>9</sup> has been found to be of the order of 10 kOe. The same order of magnitude is found in several of the orthoferrites.<sup>24</sup> If we assume that the effective field in  $\Gamma_4(F_2)$ -phase  $\text{SmCrO}_3$  is of the same order of magnitude and use the values  $m = 6.3 \text{ G}$  and  $\chi_{cc}^R = 10^{-3} \text{ emu/mole Oe}$  obtained from magnetic measurements,<sup>6</sup> we obtain  $K_b = 3.6 \times 10^2 \text{ erg/cm}^3$ ,  $|B_{55}| = 1.3 \times 10^7 \text{ erg/cm}^3$ ,  $K_u = 3.8 \times 10^5 - 11.5 \times 10^3 T \text{ erg/cm}^3$ . The value of the magnetoelastic coupling  $|B_{55}|$  is of the same order of magnitude as those found for  $\text{ErFeO}_3$ ,<sup>14</sup> and  $\text{TmFeO}_3$ ,<sup>15</sup> but the value of  $K_b$  is smaller by about two orders of magnitude. Note that the origin of the fourfold anisotropy in  $\text{SmCrO}_3$  is in the chrome–rare-earth coupling and, possibly, a two-ion anisotropy term. For  $\text{ErFeO}_3$  and

$\text{TmFeO}_3$ , on the other hand, there can be a significant contribution from single-ion anisotropy terms. We shall return to this point in Sec. IV.

In an external field  $H_a$ , the free-energy density is<sup>15</sup>

$$F_a = \frac{1}{2} K_u \cos 2\theta + K_b \cos 4\theta - \epsilon_{xz} B_{55} \sin 2\theta + \frac{1}{2} C_{55}^0 \epsilon_{xz}^2 - m H_a \sin \theta - 2 H_a (\chi_{aa}^R H_a^R + \chi_{ab}^R H_b^R) \sin \theta, \quad (8)$$

where the final term is a consequence of the chrome–rare-earth coupling. Here  $\chi_{aa}^R$ ,  $\chi_{ab}^R$  are components of the rare-earth susceptibility tensor and  $H_a^R$ ,  $H_b^R$  are the effective-field components acting on the rare-earth moments along the crystallographic  $a$  and  $b$  axes, respectively, in the  $\Gamma_2(F_x)$  configuration.<sup>23</sup> The theoretical velocity change curves calculated using Eqs. (6) and (8) for various applied magnetic fields  $H_a$  are given in Fig. 4. The characteristic temperature shift and suppression of the higher-transition-temperature dip are clearly evident and are in excellent agreement with the experimental results. The best-fit curves were obtained with

$$(m + 2\chi_{aa}^R H_a^R + 2\chi_{ab}^R H_b^R)/K_b = 1.81 \times 10^{-2} \text{ Oe}^{-1}.$$

Using the values,<sup>6</sup>  $\chi_{aa}^R = 10^{-3} \text{ emu/mole Oe}$  and  $H_a^R = 10 \text{ kOe}$ , we obtain  $(\chi_{aa}^R H_a^R / \chi_{ab}^R H_b^R) \sim 2$ , indicating that the effective Cr–Sm coupling is mostly along the  $a$  axis. This differs from  $\text{ErFeO}_3$ ,<sup>25</sup> and  $\text{TmFeO}_3$ ,<sup>15</sup> where the  $b$  axis coupling term was found to be the dominant one.

Note that, in the spin-reorientation region, the magnetocrystalline and field-induced anisotropies are at least two orders of magnitude smaller than the magnetoelastic coupling. For this reason the effect of the rotational motion on the shear wave<sup>26</sup> was not considered in our analysis. Furthermore, no detectable effect was found when the soft mode was suppressed by the external field.

(b) Shear wave propagating along the  $c$  axis, polarized parallel to  $b$ : In this geometry the shear plane is perpendicular to the rotation plane of the sublattice magnetization vectors. The magnetic anisotropy in the shear plane does not change significantly during the spin-reorientation process and therefore the energy gap between the acoustic-phonon branch and the soft modes is essentially unchanged. In this case resonant interactions are not expected to occur and indeed [see Fig. 4(a)] the experimental data do not exhibit any anomaly. A significant monotonic decrease in  $C_{44}$  was observed upon cooling below the reorientation region. The reason for this effect is not clear.

(c) Longitudinal wave propagating along the  $c$  axis: The relative velocity change for  $H = 0$  as

obtained from Eqs. (1), (3), and (5) is<sup>14</sup>

$$\frac{V}{V_i^0} = -\frac{(B_{33} - B_{31})^2}{8\rho(V_i^0)^2 K_b} (T_l \leq T \leq T_u), \quad (9)$$

$$V/V_i^0 = 0 \quad (T < T_l; T > T_u).$$

In the above expression  $\rho(V_i^0)^2 = C_{33}^0$  and  $\Delta V/V_i^0 = \frac{1}{2}C_{33}/C_{33}^0$ . From Eq. (9), no velocity shift is expected outside the spin-reorientation region, whereas, for  $T_l \leq T \leq T_u$ , the magnetoelastic-coupling term results in a reduction in the effective stiffness of the crystal. The experimental results for this sound wave mode are given in Figs. 5(b) and 5(c). Instead of the expected step-like discontinuities at the two transition end points, we see that the velocity change is spread over the reorientation region. Such a spread has been observed previously in the orthoferrites.<sup>14,15</sup> Since the spin-reorientation in  $\text{SmCrO}_3$  occurs over a very narrow temperature range the discontinuities in the velocity could not be evaluated and thus no quantitative evaluation of the magnetoelastic constants appearing in Eq. (9) could be made.

Turning to the results of the specific-heat study (Fig. 6), we have noted that a thermal anomaly is clearly evident between 33 and 35 °K. Such an anomaly is expected whenever a spin-reorientation phase transition occurs.<sup>19,27,28</sup> The center  $T_R$  of the anomaly is 1–1.5 °K higher than that found from the acoustic measurements; we attribute this to the  $\pm 1$  °K absolute accuracy in the temperature calibrations. The 2 °K width of the thermal anomaly is considerably greater than the value of 0.5 °K derived from the acoustic data and is probably a consequence of the fact that an aggregate of crystals was used for the specific heat measurement.

Due to the narrow temperature region within which the spin reorientation takes place, it was not possible to resolve the two peaks, centered at  $T_l$  and  $T_u$ , which are theoretically expected.<sup>19,27,28</sup> This was expected in view of the results of specific-heat studies on  $\text{YbFeO}_3$ ,<sup>29,30</sup>  $\text{TbFeO}_3$ ,<sup>29</sup> and  $\text{GdCrO}_3$ ,<sup>8</sup> in each of which the spin reorientation occurs within approximately 2 °K. The total entropy per mole  $\Delta S$  associated with the spin reorientation is related to the specific heat by

$$T_R \Delta S = \int C_H dT = 1.75 \pm 0.2 \text{ J/mole}, \quad (10)$$

where  $C_H$  is the specific heat at constant (zero) external field and the integral is over the area of the anomaly. Ignoring terms of order  $(T_u - T_l)/(T_u + T_l) = (T_u - T_l)/2T_R$ , it can be shown by thermodynamic arguments<sup>28,31</sup> that the  $\text{Cr}^{3+}$   $a$ - $c$  plane uniaxial anisotropy field  $H_K$  is related to  $\Delta S$  by

$$H_K = 2T_R \Delta S / 3\mu_B N, \quad (11)$$

where  $\mu_B$  is the Bohr magneton and  $N$  is Avogadro's number. Taking  $T_R = 33$  °K and substituting from Eq. (10) gives  $H_K = 2.1 \pm 0.2$  kOe. This is in good agreement with the value  $H_K = 1.7 \pm 0.1$  kOe determined in a study<sup>31</sup> of the field-induced spin reorientation in  $\text{SmCrO}_3$ .

#### IV. DISCUSSION

The results presented in the preceding sections show clearly that the  $\Gamma_2 \leftrightarrow \Gamma_4$  spin reorientation in  $\text{SmCrO}_3$  is a continuous process, involving two second-order phase transitions. The acoustic data in the spin-reorientation region were analyzed using a phenomenological model in which magnetoelastic terms linear in the strain provided the coupling between the magnetic and elastic degrees of freedom. The coupling between the chrome and rare-earth spin systems was taken into account using an effective-field approximation. The theoretical best fits obtained were in excellent agreement with the experimental results. All the observed effects, including particularly those due to external  $a$ - and  $c$ -axis magnetic fields, were reproduced satisfactorily by the model calculations, confirming the continuous nature of the spin reorientation. The expected anomaly in the specific heat was also observed.

The central question is why the spin reorientation is continuous in  $\text{SmCrO}_3$  (and, possibly, in  $\text{GdCrO}_3$ ),<sup>7,8</sup> but discontinuous in  $\text{ErCrO}_3$ ,<sup>3</sup> and  $\text{NdCrO}_3$ .<sup>4</sup> This problem has been considered in particular by Yamaguchi<sup>22</sup> in his theoretical study of spin reorientation in the orthochromites and orthoferrites. He concludes that  $\Gamma_4 \rightarrow \Gamma_2$  (with decreasing temperature) transitions should indeed be continuous in these compounds while both  $\Gamma_4 \rightarrow \Gamma_1$  ( $\text{ErCrO}_3$ ,  $\text{DyFeO}_3$ )<sup>11</sup> and  $\Gamma_2 \rightarrow \Gamma_1$  ( $\text{NdCrO}_3$ ) transitions will occur abruptly. However, magnetization<sup>31,32</sup> and neutron-diffraction<sup>33</sup> measurements have shown that the  $\text{DyFeO}_3$   $\Gamma_2 \rightarrow \Gamma_1$  spin reorientation is rotational in character and, in fact, takes place over a rather wide temperature range (from approximately 60 to 20 °K). In addition, the incomplete low-temperature  $\Gamma_2 \rightarrow \Gamma_1$  transition in  $\text{ErFeO}_3$  is rotational in character.<sup>34–36</sup>

It thus appears that an essential element in understanding why a given transition is continuous or abrupt, in addition to the specification of the two end phases, is the source of the effective fourfold anisotropy coefficient  $K_b$  [see Eq. (1)]. Here there is a significant difference between orthoferrites and orthochromites as  $K_b$  will have a single-ion contribution for  $\text{Fe}^{3+}$  ions with  $S = \frac{5}{2}$ , but not for the  $S = \frac{3}{2}$  spins of  $\text{Cr}^{3+}$  ions. While a

Cr-only fourfold anisotropy term can, in principle, arise from a two-ion or ion-pair mechanism, this is not expected to be significant in  $R\text{CrO}_3$  compounds where no crystallographic pairing of  $\text{Cr}^{3+}$  ions occurs. Thus, for the orthochromites, one must consider not only the contribution of the rare-earth spin system to the effective twofold anisotropy coefficient  $K_u$ , but also its contribution to  $K_b$ . This has recently been done by Gordon.<sup>31</sup> His analysis confirms that the  $\Gamma_4 \leftrightarrow \Gamma_2$  spin reorientation in  $\text{SmCrO}_3$  (and also the  $\Gamma_4 \leftrightarrow \Gamma_1$  reorientation in  $\text{DyFeO}_3$ ) can be rotational in character, in agreement with the results of our acoustic-velocity

and specific-heat measurements.

In conclusion, we have here presented conclusive evidence that the spin-reorientation phase transition in  $\text{SmCrO}_3$  is second order in character. While common in the orthoferrites, this is the first time that rotational rather than abrupt behavior has been shown to occur in the rare-earth orthochromites.

#### ACKNOWLEDGMENT

We are indebted to J. D. Gordon for several helpful discussions.

\*Supported in part by a grant from the United States-Israel Binational Science Foundation (BSF), Jerusalem, Israel.

<sup>1</sup>S. Geller, *Acta Crystallogr.* **10**, 243 (1957); S. Quezel-Anbrunaz and M. Mareschal, *Bull. Soc. Fr. Miner. Crystallogr.* **86**, 204 (1963).

<sup>2</sup>E. F. Bertaut, J. Mareschal, G. de Vries, R. Aleonard, R. Pauthenet, J. P. Rebouillat, and J. Sivardière, *IEEE Trans. Magn.* **2**, 453 (1966).

<sup>3</sup>See A. Hasson, R. M. Hornreich, Y. Komet, B. M. Wanklyn, and I. Yaeger, *Phys. Rev. B* **12**, 5051 (1975), and references cited therein.

<sup>4</sup>See R. M. Hornreich, Y. Komet, R. Nolan, B. M. Wanklyn, and I. Yaeger, *Phys. Rev. B* **12**, 5094 (1975), and references cited therein.

<sup>5</sup>K. Tsushima, K. Aoyagi, and S. Sugano, *J. Appl. Phys.* **41**, 1238 (1970); K. Tsushima and T. Tamaki, *Proceedings of the International Conference on Ferrites, Kyoto, 1970* (University Park, Baltimore, 1971), p. 383.

<sup>6</sup>I. Yaeger, Ph.D. thesis (Weizmann Institute of Science, 1973) (unpublished).

<sup>7</sup>K. Tsushima and T. Tamaki, *International Conference on Magnetism, Moscow, 1973* (unpublished).

<sup>8</sup>A. H. Cooke, D. M. Martin, and M. R. Wells, *J. Phys. C* **7**, 3133 (1974).

<sup>9</sup>T. Tamaki, K. Tsushima, T. Matsui, and H. Nishimura [International Conference on Magnetism, Amsterdam, 1976 (unpublished)] have reported a spontaneous spin reorientation in  $\text{TmCrO}_3$ . This has not been observed elsewhere; see R. M. Hornreich, B. M. Wanklyn, and I. Yaeger, *Int. J. Magn.* **4**, 313 (1973).

<sup>10</sup>L. M. Levinson, M. Luban, and S. Shtrikman, *Phys. Rev.* **187**, 715 (1969).

<sup>11</sup>For a review, see R. L. White, *J. Appl. Phys.* **40**, 1061 (1969).

<sup>12</sup>S. M. Shapiro, J. D. Axe, and J. P. Remeika, *Phys. Rev. B* **10**, 2014 (1974).

<sup>13</sup>G. Gorodetsky, and B. Luthi, *Phys. Rev. B* **2**, 3688 (1970).

<sup>14</sup>G. Gorodetsky, B. Luthi, and T. J. Moran, *Int. J. Magn.* **1**, 295 (1971).

<sup>15</sup>G. Gorodetsky, S. Shaft, and B. M. Wanklyn, *Phys. Rev. B* (to be published).

<sup>16</sup>B. M. Wanklyn, *J. Cryst. Growth* **5**, 323 (1969).

<sup>17</sup>T. J. Moran and B. Luthi, *Phys. Rev.* **187**, 710 (1969).

<sup>18</sup>A. de Combarieu, J. Mareschal, J. Michel, J. Peyrard, and J. Sivardière, *C. R. Acad. Sci. (Paris)* **267**, 1169 (1968).

<sup>19</sup>H. Horner and C. M. Varma, *Phys. Rev. Lett.* **20**, 845 (1968).

<sup>20</sup>T. J. Beaulieu, Microwave Laboratory Report No. 1530, Stanford University (unpublished).

<sup>21</sup>A. Berton and B. Sharon, *J. Appl. Phys.* **39**, 1367 (1968).

<sup>22</sup>T. Yamaguchi, *J. Phys. Chem. Solids* **35**, 479 (1974).

<sup>23</sup>E. F. Bertaut, in *Magnetism*, edited by G. T. Rado and H. Suhl (Academic, New York, 1963), Vol. III, p. 149.

<sup>24</sup>D. Treves, *J. Appl. Phys.* **36**, 1033 (1965).

<sup>25</sup>D. L. Wood, L. M. Holmes, and J. P. Remeika, *Phys. Rev.* **185**, 689 (1969).

<sup>26</sup>R. L. Melcher, in *Proceedings of the International School of Physics, Enrico Fermi Course, LII, Varenna, 1971*, edited by E. Burstein (Academic, New York, 1973).

<sup>27</sup>J. Sivardière, *Solid State Commun.* **7**, 1555 (1969).

<sup>28</sup>L. M. Levinson and S. Shtrikman, *Solid State Commun.* **8**, 209 (1970).

<sup>29</sup>J. Peyrard and J. Sivardière, *Solid State Commun.* **7**, 605 (1969).

<sup>30</sup>M. R. Moldover, G. Sjolander, and W. Weyhmann, *Phys. Rev. Lett.* **26**, 1257 (1971).

<sup>31</sup>J. D. Gordon, Ph.D. thesis (Weizmann Institute of Science, 1976) (unpublished).

<sup>32</sup>L. Holmes, L. G. Van Uitert, and R. Hecker, *J. Appl. Phys.* **42**, 657 (1971).

<sup>33</sup>H. Pinto and H. Shaked (private communication).

<sup>34</sup>G. Gorodetsky, R. M. Hornreich, I. Yaeger, H. Pinto, G. Shachar, and H. Shaked, *Phys. Rev. B* **8**, 3398 (1973).

<sup>35</sup>V. M. Khmara, N. M. Kovtun, and G. A. Troitskii, *Solid State Commun.* **15**, 1769 (1974).

<sup>36</sup>F. Vigneron, *J. Phys. (Paris)* **37**, 103 (1976).